Heavy-ion test of detectors with conventional and resistive Micromegas used in TPC configuration

Jean-Éric Ducret[a], Philippe Legou[a], Jerzy Łukasik[b], Alain Boudard[a], Michel Combet[a], Bronisław Czech[b], Robert Durand[a], Thomas Gorbinet[a], Pascal Le Bourlout[a], Sylvie Leray[a], Vladislav Matousek[c], François Nizery[a], Piotr Pawłowski[b], Marie-Delphine Salsac[a], Orlin Yordanov[d]

[a]*Commissariat à l'Energie Atomique, IRFU, F91191 Gif sur Yvette France*
[b]*Institute of Nuclear Physics, IFJ-PAN, ul. Radzikowskiego 152, 31-342 Kraków, Poland*
[c]*Institute of Physics, Slovak Academy of Sciences, Dubravska cesta 9, 854 11 Bratislava, Slovakia*
[d]*Institute of Nuclear Research & Nuclear Energy, Bulgarian Academy of Sciences, 72, Tzanigradsko chaussee Blvd, BG-1784 Sofia, Bulgaria*

Abstract

We have performed tests of Micromegas detector prototypes using the heavy-ion beams from the SIS synchrotron of GSI (Darmstadt, Germany). The beams varied from $^{12}C^{6+}$ to $^{179}Au^{65+}$ and from 250 to 1000 MeV per nucleon. We have tested two amplification technologies, conventional and resistive Micromegas, and two construction concepts, bulk-Micromegas and micro-meshes screwed on the PCB. The obtained position resolution below 200 μm for 5 mm wide strips implies, that the bulk resistive Micromegas technology might meet the requirements of the future R3B TPC project. We also developed a fast and very low noise front-end electronics connected directly to the Printed Circuit Board (PCB) of the detector itself. This concept has shown very good performances and robustness.

Key words: Gaseous detectors, TPC, Micromegas, Resistive readout, Low-noise preamplifier

1. Introduction

Within the international FAIR project, the R3B collaboration (Reaction studies with Radioactive Relativistic beams) will be in charge of the physics program with secondary beams of energy between 200 and 1500 MeV per nucleon. Central to the R3B set-up will be a large-aperture superconducting magnet under construction at CEA-Saclay. A European collaboration has been formed to work on the design of a large time-projection chamber (TPC) to be installed behind this magnet to cover the full phase-space of the charged fragments produced in the target. Within this collaboration, we have performed tests of detector prototypes with the heavy-ions beams at GSI Darmstadt. These prototypes were equipped with a gaseous Micromegas [1] detector. We have tested two amplification technologies, either conventional or resistive Micromegas [2] and two construction concepts, bulk-Micromegas or micro-meshes screwed on the PCB. The resistive Micromegas exhibit a major interesting feature for our application: a large transversal and in-time spread of the heavy-ion signals, making possible a linear amplification and collection of huge signals.

The future R3B TPC will have to provide particle identification and kinematics reconstruction for the detected charged reaction products. The charge identification has to be done from protons (Z=1) to uraniums (Z=92) by integration of the energy loss along the track inside the active volume of the detector. On an event by event basis and for each fragment, it will also provide the tracking information (position in three dimensions). This detector will have a modular design and should be 8 m long (see Fig. 1) to cover the final-state phase space of both small and large rigidity fragments. Each module will be composed of a central, horizontal cathode and two Micromegas detectors on opposite sides. Utilization of a TPC guarantees minimum amount of material on the way of the beam, minimizing multiple scattering effects and parasitic interaction with the detector. The necessary position resolution aimed at to reconstruct momenta at the 10^{-3} level and angles at the reaction point with an accuracy of 1 mr (RMS) is $\simeq$ 200 μm.

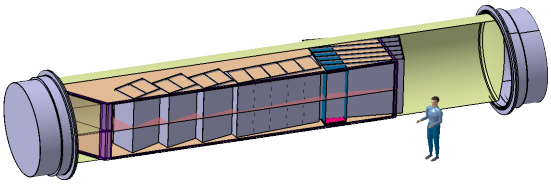

Figure 1: Design layout of the future R3B TPC

This TPC can be seen as a large dimension gas enclosure (8 m long and 2.4 m diameter, see Fig. 1) with a thin window as the physics requires a very low opacity to particles (< 1%). Moreover, other constraints like maintenance, accessibility to the detectors and to the electronics, modularity (to reduce costs) have to be taken into account for the design of such a large device. To avoid handling large entrance and exit windows during the maintenance, we preferred to design a gas enclosure with a flexible and foldable envelope. In the case of a rigid enclosure, sealing around the Micromegas detectors is achieved with an O-ring that rests on ties. A flexible enclosure made with

PET allows to withdraw such ties and stays easily collapsible. It can be folded and stored in the extremities of the enclosure away from the particle tracks. This solution allows also to reduce the risk of leakage since we will use very few seals (only at both ends). Moreover designing detection modules unsealed will make possible to work with cheaper technologies.

2. Beam tests

For the beam tests we have built six small prototypes of TPCs in order to test their tracking performance. All prototypes consisted of plastic boxes with thin entrance and exit windows. Four chambers were equipped with 48 "narrow" strips, 40 (length) $\times$ 0.835 (width) mm^2 and 65 μm spacing. Three of these prototypes were equipped with standard readout pads, for measurement of the direct charge deposit, and one of them was built utilizing the new resistive Micromegas technology allowing for charge dispersive readout. The two other chambers were equipped with 7 "wide" strips of 5 mm width and 150 μm pitch, both based on the resistive Micromegas technology.

Meshes of Micromegas detector are realized at CERN [3]. They are made of a 100 μm copper-plated Kapton foil, with 5 μm of copper (see Fig. 2). Spacers of 100 μm height realize the amplification gap of the Micromegas.

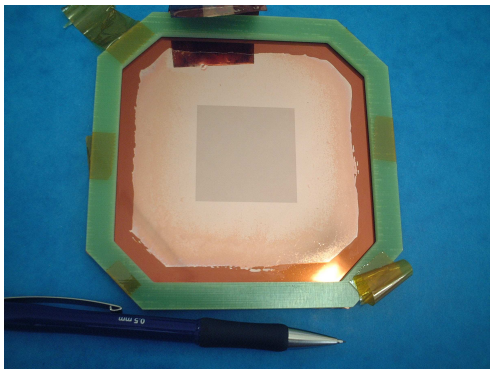

Figure 2: A picture of 100 μm gap mesh.

Another way to make a Micromegas detector is to realize a "bulk". In this case the mesh can be seen as additional layers of the PCB. It is obtained by lamination of a woven grid on an anode with a photo-imageable film. It is a ready-to-use solution with no frame anymore and no mounting operations required. Moreover, this technology allows to produce meshes of large area. This will be the preferred solution for the final R3B TPC.

For the R3B TPC project, and for large detectors in general, it is essential to reduce as much as possible the number of electronics channels in order to reduce the price, i.e. to work with strips or pads as wide as possible. In the resistive technology, by adding a resistive foil on the strips, we can spread the charge over several strips which improves the reconstruction of the track position. The signal on the neighbouring strips is larger due to the RC dispersion. Furthermore, such a spread is favourable, in principle, to reduce the probability of discharge on the micro-mesh.

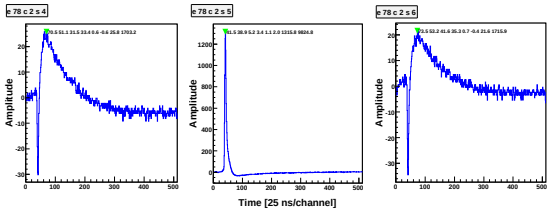

Figure 3: Response of three 5 mm wide strips in resistive readout technology.

Fig. 3 shows the response of three neighbouring strips in resistive readout technology. The similarity of the left and right neighbours indicates that the track was crossing the chamber exactly above the middle of the central strip. The response of this strip is very sharp while the responses of the neighbours are much broader and much smaller (note the different scales). The amplitudes of the neighbours amount to about 2% of the amplitude of the middle strip, while their integrals amount to about 17%. This was the reason why we decided to use integrals as weights to calculate the weighted hit positions in case of chambers with wide resistive pads. Thus, resistive readout allows to improve the position resolution, but on the other hand, when looking at the duration of the neighboring pulses (~12 μs), this may be a limitation in case of a real experiment, in high track density regions. In this case, i.e. in the presence of multi-hits, the information from neighbouring pads may be of little value. The gas used for the test beam was P10 (90% argon, 10% methane).

In order to read each channel of the detectors, we developed a special front-end module called Antioche [4], see Fig. 4. Each strip on the mother board of the detector is fed by an Antioche. The size of each module is 22 $\times$ 20 mm^2.

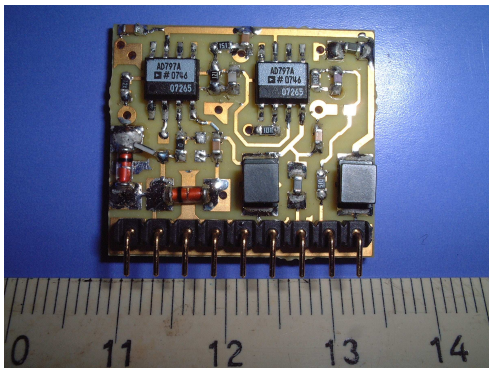

Figure 4: Antioche preamplifier card.

Each Antioche houses a spark protection and a double stage of a very fast and low noise voltage preamplifier. The noise measured at the output of the preamplifier is lower than 100 μV RMS. Each channel was read out by a 14 bit 40 MS/s FADC, which allowed to store the whole waveforms for the off-line analysis. The mother board houses the strips of the detector, power supplies and the preamplifier cards, thus the electrical architecture is simple and at the end leads to a very low noise in running conditions. It is important to notice that there is no crosstalk between channels on the Printed Circuit. Fig. 5 shows

an example waveform provided by the Antioche preamplifier. The pulse consists of a fast (~10 ns wide) and a slow (~80 ns wide) component. Unfortunately, such fine structures could not be viewed using 40 MS/s digitizers.

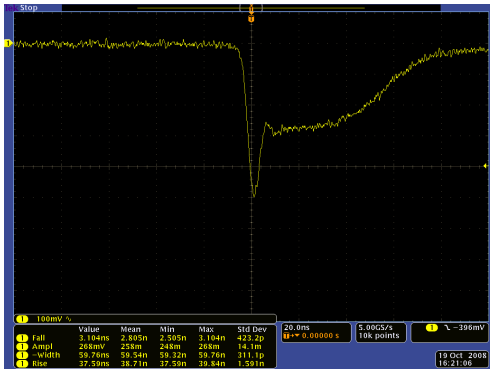

Figure 5: Micromegas signal readout by Antioche after 20 m coaxial cable.

3. Results

The beam test of April 2009 was carried out in the test area of Cave C at GSI-Darmstadt. The setup is presented in Fig. 6. Six prototype chambers were placed between two pairs of scintillators (paddles of 10×10 cm^2 active areas or "fingers": 10 cm long and 1×1 cm^2 wide), which were used to provide the DACQ trigger. The beam was Au^{65+} (not fully stripped) at 250 MeV per nucleon.

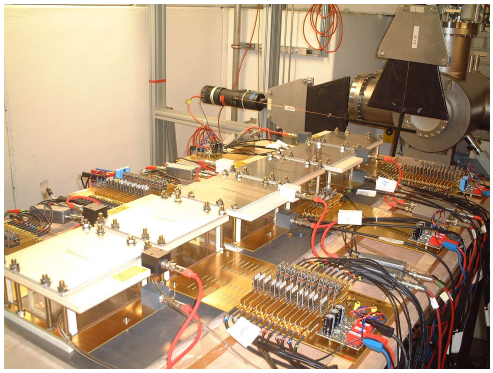

Figure 6: View of the test setup. Projectiles come out of the beam pipe visible at the top right corner, behind the scintillator cross.

Fig. 7 shows an event display with a reconstructed track in the frame where z represents the beam direction, x is the pad tracking direction and y (not shown) is the drift direction. The gray boxes represent the active strips (pads), while the superimposed histograms ("hits") represent the amplitudes (for narrow strips) or integrals (for wide strips) of the registered peaks. In particular, the chamber (pad row) marked with "R 835" shows the effect of resistive readout, causing a wider range of strips to respond to the passing projectile. For the standard readout, this range is limited by the width of the electron cloud. The drift distance was typically about 4-5 cm.

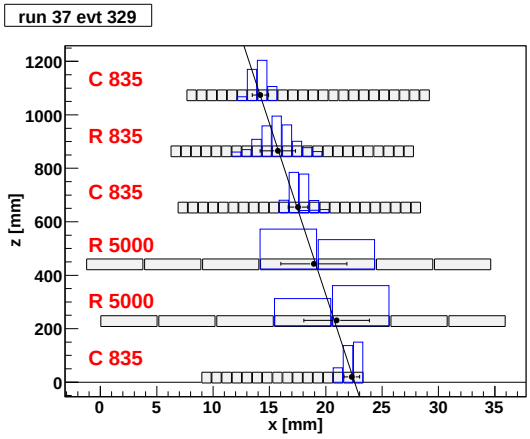

Figure 7: Event display with a reconstructed track. The beam goes from bottom to top. *C* and *R* label the Classical and Resistive readout chambers, respectively.

Small misalignments of individual chambers have been corrected off-line using a double least square approach. One least square allowed to get the optimal parameters of each individual track, while the other was applied to obtain the offsets minimizing the sums of squared distances between the hit position and the track for each chamber, using the whole statistics. The track parameters were obtained from the other chambers, excluding the one of interest. This routine reduced to solving a set of six linear equations with the constraint that two of the chambers have fixed positions. The offsets thus obtained were smaller than 2.3 mm. Fig. 8 shows the distribution of residuals (distances between the estimated hit position and the fitted track) before and after the software alignment.

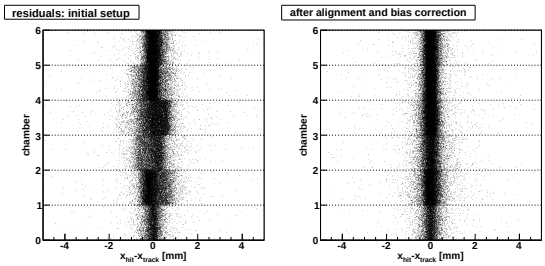

Figure 8: Distribution of residuals before and after software alignment.

The residuals showed also some systematic dependence along the pad plane (see Fig. 9 - left panel). We have corrected for these offsets using similar method as described in [5]. The right panel of Fig. 9 shows the remaining bias after correction. The distortions were found to increase with the HV applied to the mesh and might be possibly related to the lack of the field collimator.

Fig. 10 shows the pad response functions, PRF, for individual strips of three chambers. The plots represent relative amplitudes of individual strips as a function of their distances from the track. The PRFs for the 835 μm strip standard readout chamber (top) are narrower than those of resistive Micromegas chambers. In the case of narrow strip chambers one can observe the evolution from symmetric shapes in the middle to

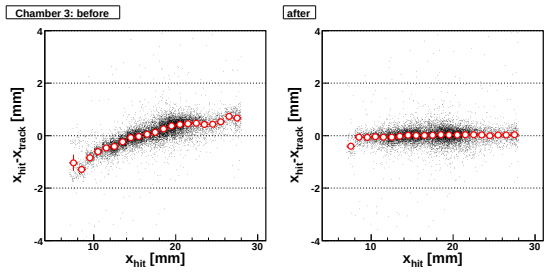

Figure 9: Pad response corrections.

more asymmetric ones further away from the center (edge effects responsible for the deviations from Fig. 9). Single strip hits are excluded from the plot. Note that the PRFs widen as the HV is increased in the mesh, which is linked to an increase of the average multiplicity of fired pads.

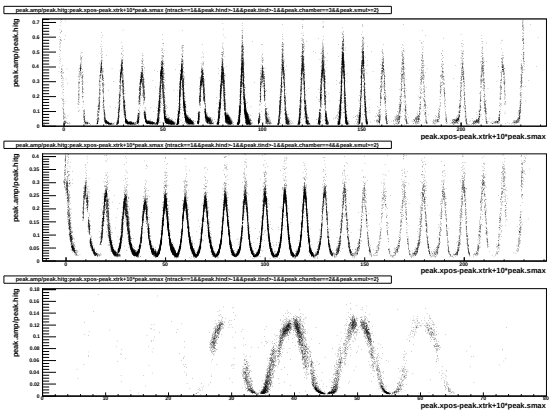

Figure 10: Pad response functions for individual strips of narrow strip classical (top), narrow strip resistive (middle) and wide strip resistive (bottom) chambers.

In order to measure the position resolution of the chambers we have selected a set of tracks with a drift distance of about 5±0.5 cm and with small angles ($\theta < 0.7°$). Fig. 11 shows the single-strip resolutions, i.e. the resolutions for a selected strip with maximum statistics, provided that this strip had the maximum amplitude.

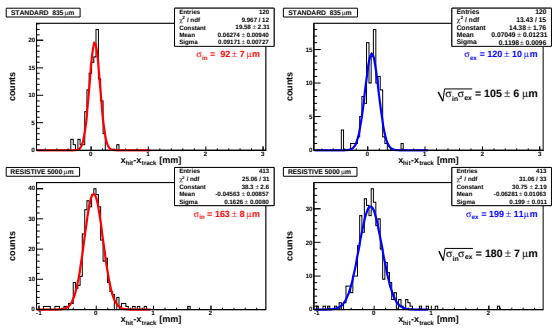

Figure 11: Single strip resolution for narrow strip standard readout chamber (top) and wide strip resistive readout chamber (bottom). Left and right panels show the results for σ_{in} and σ_{ex} (see text).

The obtained resolutions (from Gaussian fits) are specified in the respective panels. Obviously, resolutions obtained by including the chamber of interest in the track fit are overestimated due to autocorrelations, and those obtained by excluding it are underestimated. A compromise proposed by [6, 7] is a geometric-mean recipe. Resolutions obtained this way are: $\sqrt{\sigma_{in}\sigma_{ex}}$ = 105±6 μm for a narrow strip chamber with classical readout, and 180±7 μm for a wide strip chamber and resistive readout. Here, σ_{in} and σ_{ex} are obtained by computing the track resolution by including, respectively excluding the chamber of interest from the track fit. More representative and meaningful are resolutions obtained for the whole chamber, i.e. including all strips:

CHAMBER	$\sqrt{\sigma_{in}\sigma_{ex}}$
835 μm Standard	159±3 μm
835 μm Resistive	154±3 μm
5000 μm Resistive	180±5 μm

The results demonstrate that, using wider pads with resistive readout, one can still measure positions with a resolution comparable to that obtained using 5 times narrower strips and classical readout. Another interesting observation is that resistive readout applied to narrow strips does not significantly improve the resolution. Notice that these results agree well with previous measurements on conventional MicroMegas we performed with a ^{12}C at 1 GeV per nucleon and with $^{58}Ni^{28+}$ at 600 MeV per nucleon, i.e. with smaller primary ionisation signals.

4. Conclusion

It appears after our beam tests that a TPC equipped with a Micromegas detector could be the answer for tracking and particle identification in heavy-ion collisions. As a matter of fact taking into account the transport properties of the magnet and the multiple scattering from the target point to the detector, the position reconstruction in this TPC has to be performed with a resolution of 200 μm. With strips of 5 mm width we obtained a space resolution of better than 200 μm. Moreover, this test was performed successfully with a particle flux which is much higher than that we will have in the final detector, where the track density will be rather low, what permits the use of rather wide pads.

The new resistive Micromegas technology seems to fit very well in our application allowing the reduction of the number of electronics channels which is very important for such a big detector. Nevertheless beam tests have to be performed in future for testing the energy resolution, position resolution as a function of the drift length and mainly the charge resolution in the real experiment with the target. Furthermore, in order to reduce as much as possible the number of channels in the final detector, we will have to test 10 mm and 20 mm wide pads.

References

[1] Y. Giomataris *et al.*, Nucl. Instr. and Meth. A 376 (1996) 29.
[2] M.S. Dixit *et al.*, Nucl. Instr. and Meth. A 518 (2004) 721.
[3] R. de Oliveira, Nuclear Science Symposium, Portland, Oregon, 19-25 September 2003.
[4] Ph. Legou *et al.*, note CEA(2010).
[5] K. Boudjemline *et al.*, Nucl. Instr. and Meth. A 574 (2007) 22.
[6] R.K. Carnegie *et al.*, Nucl. Instr. and Meth. A 538 (2005) 372.
[7] D.C. Arogancia *et al.*, Nucl. Instr. and Meth. A 602 (2009) 403.